Case study: 7-8 Oc 2012t

15 Oct 2012

1 Introduction

Although the term "cold pool" is well defined for deep basins, craters and sink holes, the term "shallow cold pool" is less clear since these smaller scale phenomena are often more nonstationary and are more significantly influenced by the large-scale flow, regional flows and small scale motions such as gravity waves. Shallow cold pools, such as at the SCP (Shallow Cold Pool) site, often include weak down-gully flow and thus could also be referred to as very slow drainage flows. A map of the network of stations is provided in the Appendix at the end of the document.

The following report examines the night 07-08 October 2012. During this night, the flow in the gully is constantly modulated by the nonstationary ambient flow above the gully. The ambient flow can eliminate the gully flow in the upland gullies and strongly influence the flow in the main gully. The wind vector in the gully is frequently shifted to the substantial cross gully component although the cold air (stratification) is not eliminated.

2 Evolution of the vertical structure

For 07-08 October, rapid cooling begins at the surface at about 00Z (1700 MST) (Figure 1). This cooling is slower at the top of the tower as is normally the case for nocturnal boundary layers. Although the cooling is generally most rapid in the early evening, on this night, the surface cooling essentially decreases after 2100 MST, probably because of increasing wind speed (Figure 2). The temperature roughly oscillates on various time scales about a constant temperature. The temperature difference between the top and the bottom of the tower is near 8 K throughout the night. The termination of the rapid cooling occurs with a reversal from southerly to southwesterly flow

at the surface and southerly to westerly at the top of the tower (Figure 3). Rapid acceleration begins several hours after the onset of the westerly flow peaking with winds near 6 m/s at the top of the tower. Although the increased wind speed does not lead to warming, if may have prevented further nocturnal cooling.

The oscillations of the temperature and wind field will be examined in more detail later in a separate document.

The upper panel of Figure 5 compares sonic-anemometer temperatures with those from the slow-response temperature (black). The reversal of the stratification around 3 m in the sonic temperature profile (red) could be due to an offset. However, the slow response temperature shows a hint of a perturbation as well. Is there a preferred layer of eddy overturning? The middle panel compares the speed profiles from the Campbell sonic anemometers and the Handar sonic anemometers. Within the resolution of the data, the profiles compare well. There appears to be a slight perturbation in the wind profile near the level (or just above) of the temperature gradient reversal. The lower panel compares wind direction. There is distortion in the sonic wind direction profile near the surface but only with an amplitude of 1 degree. This could be due to alignment issues, flow distortion or could be real. The lower panel shows a 5-10 degree difference between the Campbell and Handar directions.

2.1 A cold event

We arbitrarily examine the vertical structure of the first surface cooling event at 2030 MST in more detail (upper panel of Figure (4). Strong stratification occurs in the lowest 10 m where the flow is SW flow. The flow abruptly shifts with height to NNE at 10 m and above. The very weak wind speed decreases with height and reaches a minimum at 5 m. The local maximum of the measured wind speed at 0.5 m implies that the flow is weak maximum around 0.5 m or below. The turbulence is very weak but increases with height throughout the tower layer.

The local reversal in the temperature profile between 3 and 4 m is under investigation. This reversal also occurs in the profile averaged over the entire night (red, upper panel, Figure 5). A small perturbation occurs in the slow-response temperature profile (black).

The lower panel of Figure 4 shows an arbitrary example of the profiles between cold events. The stratification is actually weaker in the lowest 10 m

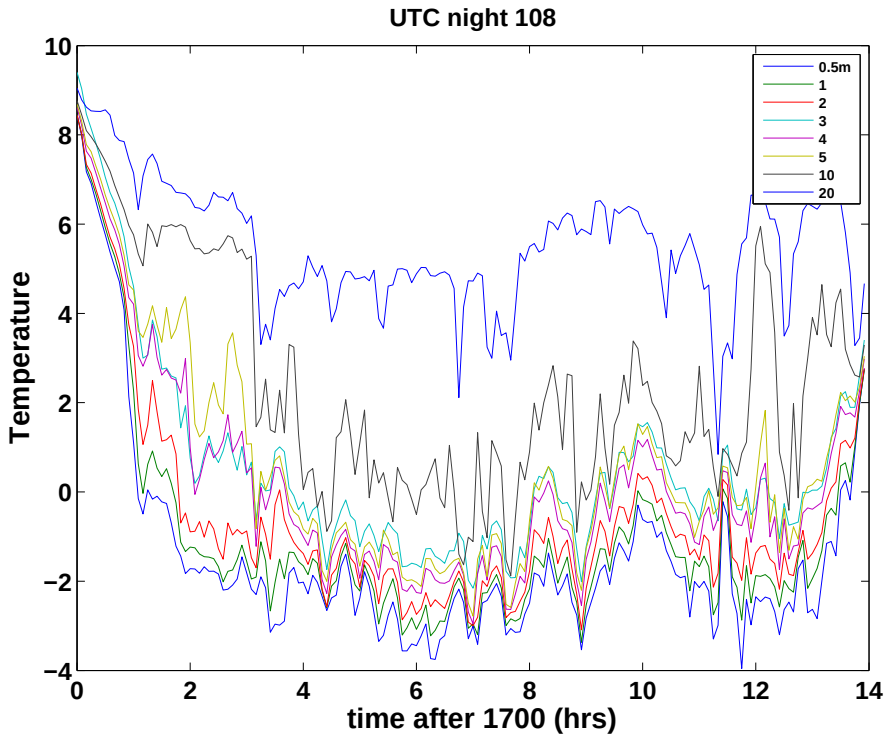

Figure 1: Five-minute averaged sonic anemometer temperature on the main tower for the 8 levels, 0.5, 1, 2, 3, 4, 5, 10, 20 m.

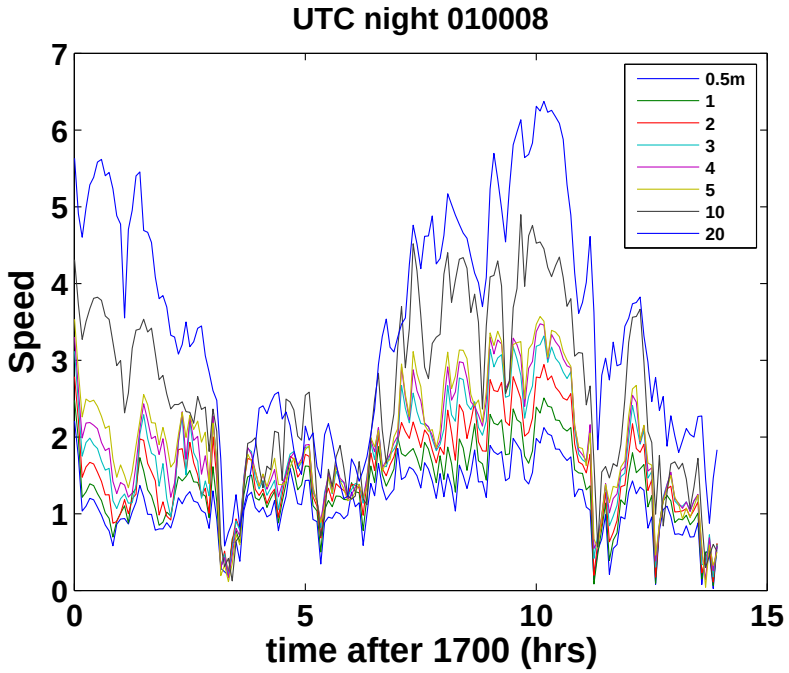

Figure 2: Evolution of nocturnal wind speed for the eight levels of sonic anemometers on the main tower.

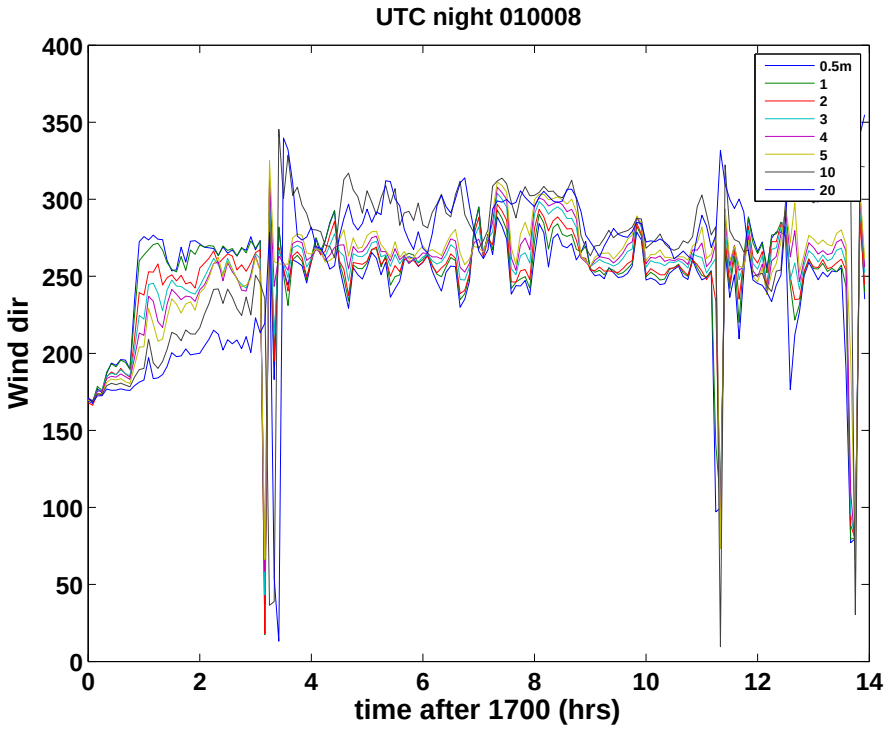

Figure 3: Evolution of the wind direction for the eight levels of sonic anemometers on the main tower.

implying formation of a thin partially mixed layer within the stratified flow. Reduced shear near the surface leads an overlying inflection point. The flow is westerly at all levels.

The Handar and Campbell wind speeds compare well considering the limited vertical resolution (middle panel, Figure 5). The directions deviate by 5-10 degrees although final corrections in orientation have not been applied.

2.2 Wind maxima

The wind speed maximum sometimes occurs below the 20-m level (blue, Figure 6) defining a low-level weak "jet". The nearly vertical blues lines indicate when the low-level wind maximum is below 20 m often to 10 m but sometimes lower. The low-level wind maxima are more prevalent when defined in terms of the lowest 10 metres (black). That is, a near-surface wind maximum may be weaker than the 20 m wind but stronger than the 10 m wind. Identifying wind maximum in terms of any decrease of wind speed between adjacent levels identifies even more wind maxima. Here, we define the height of the wind maxima in terms of the bottom of the lowest layer where the shear reverses to negative (red, Figure 6), if such a reversal occurs. In terms of the discrete levels, the height of the wind maximum is approximated by the bottom of the lowest layer where the wind speed decreases upward across the layer by more than 0.1 ms^{-1}. This will be referred to as the "bottom-up" approach.

For most of the night, the maximum speed occurs at the top of the tower (blue line at 20 m) except for the 3-4hour period starting around 2000 MST. After midnight, the wind maximum is always at the top of the tower. A few intermittent cases occur where the wind maximum in the lowest 10 m is below 10 m. (black line below 10 m or red line exists due to shear reversal).

Consider the 3 hour and 15 minute period ending about midnight where low-level wind maxima occur intermittently (Figure 7). The individual profiles are characterized by a wide variety of vertical structures. The mean speed profile (thick black) occurs with only a weak maxima at about 4 m. With such nonstationary conditions, the mean turbulence is probably not well predicted by the mean wind profile since much of the turbulence may generated by significant deviations from the mean wind profile in a nonlinear manner (for example the shear exceeds a threshold for instability). The maximum turbulence vertical velocity variance occurs above the weak maximum. In contrast, the vertical velocity variance increases with height at all levels

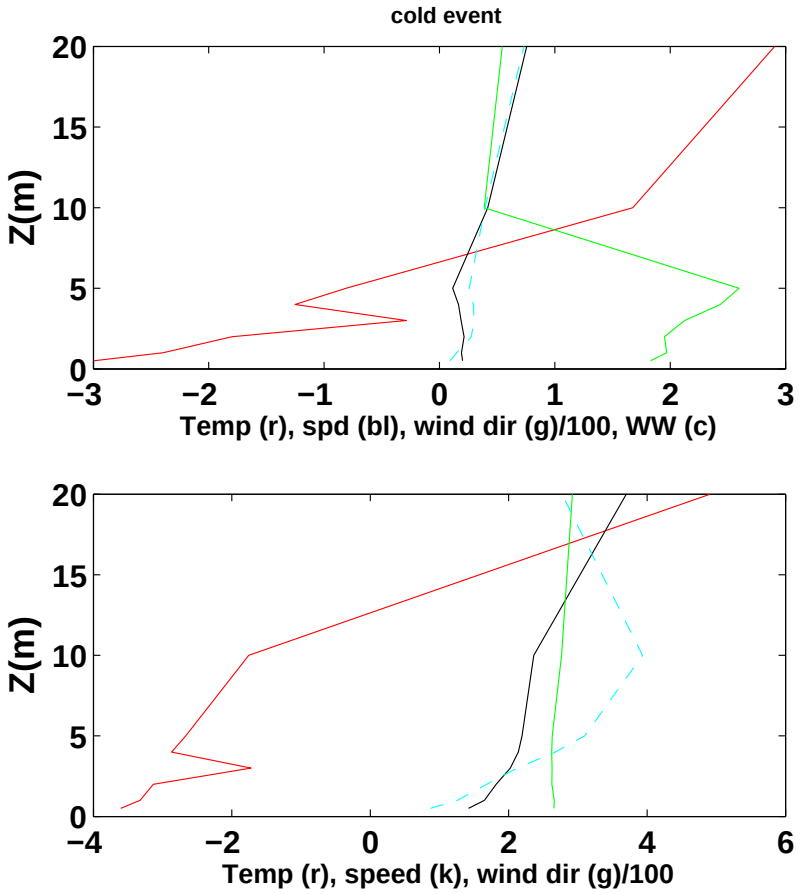

Figure 4: Profiles for a cold air event (upper) and between cold air events (lower) for the the temperature from the sonic anemometer (red), the corresponding wind speed (black), the wind direction/100 (green) and the vertical velocity variance (cyan dashed),

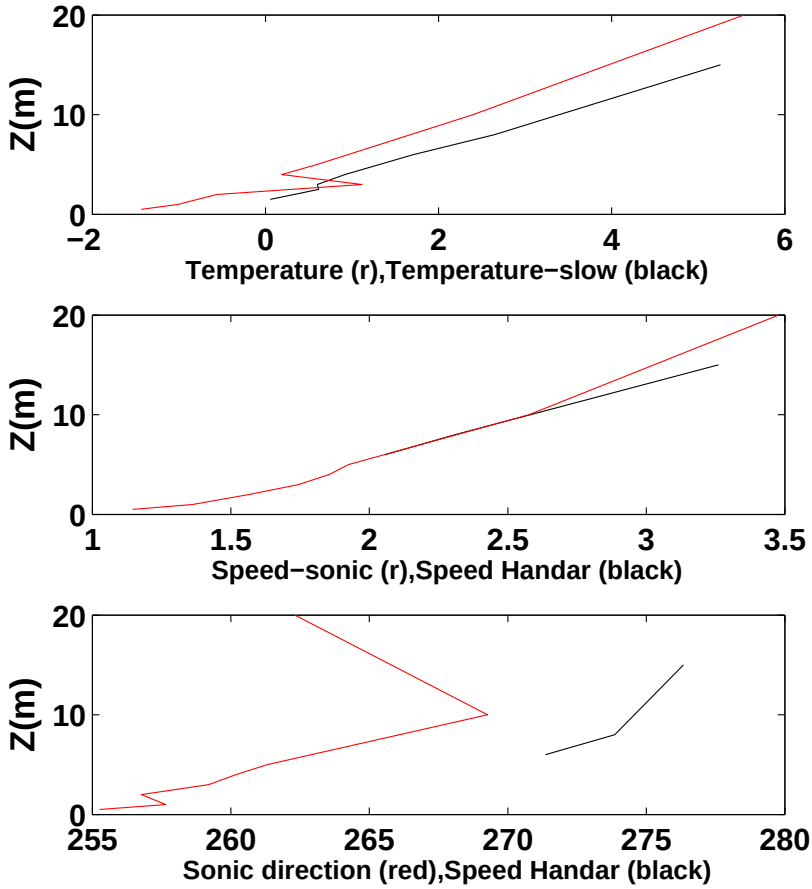

Figure 5: Comparison of profiles averaged over the night based on Campbell Csat sonic anemometers (red), Handar sonic anemometers (black) and the slow response temperature (black). Wind components are averaged over the night before computing wind directions.

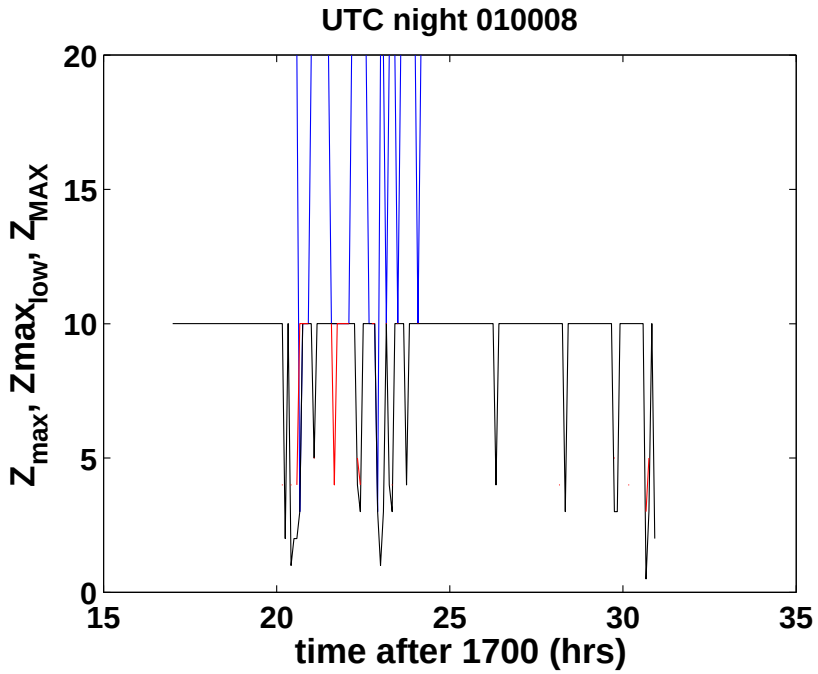

Figure 6: Height of the maximum wind speed in the lowest 20 m (blue), in the lowest 10 m (black), the bottom-up estimate of the wind maximum (red).

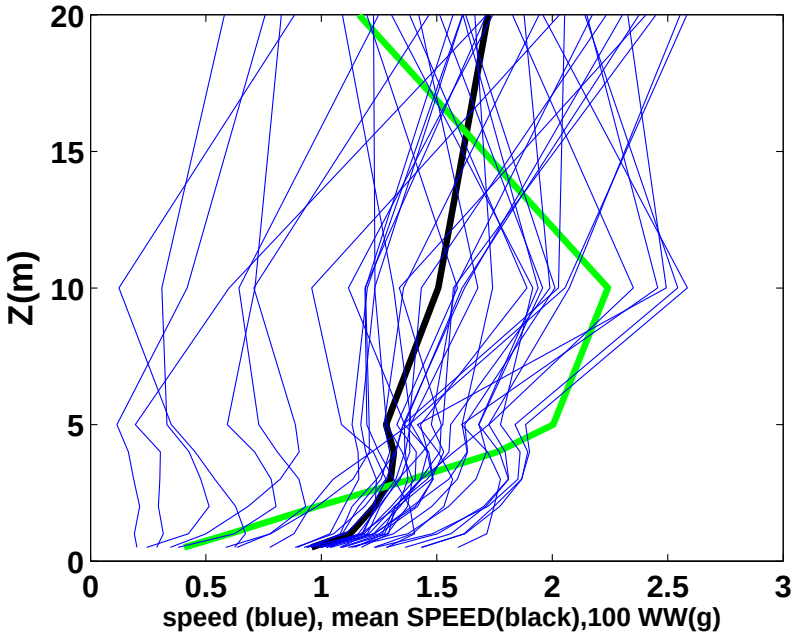

Figure 7: Vertical profiles of the 5-minute wind speed (blue lines), the average over the 3 hr 15 min period (black) and the corresponding average of 100 $\times$ ww (green).

for periods with no low-level wind maximum (not shown). While such an increase is typical of very stable conditions, the increase of turbulence with height in the gully may be augmented by advection of turbulence from the windier higher ground.

Inspection of individual profiles indicates that the turbulence is often largest in the general vicinity of an inflection point separating the underlying negative curvature and positive curvature associated with the minimum above the wind maxima. However, the curvature is difficult to quantify from discrete wind profiles. Furthermore, the wind profile and turbulence profile may be out of phase and examination of their coupled evolution requires following the flow in a Lagrangian framework.

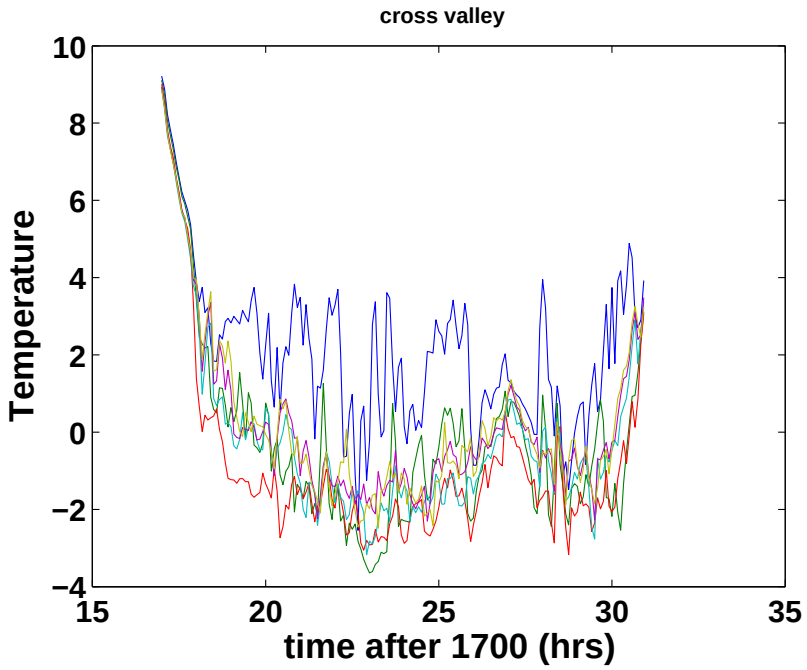

Figure 8: The time series of the cross-valley variations of 0.5-m slow-response temperature for stations 9 (blue), 10 (blue-green) , 11 (red), 12 (green-blue), 13 (violet), and 14 (grey).

2.3 Horizontal variation

The cross-valley temperature distribution (Figure 8) shows expected coldest temperatures at the valley bottom, and warmest temperature at the top of the side slopes (grey and blue). Station 9 values seem anomalously warm. This particularly warm air is verified by the slow response temperature at 0.5 m and 2 m and is probably related to a northerly flow component through the buildings at the top of the slope.

The temperature along the gully axis is warmest at station 1 in the source region (yellow, Figure 9). The air also tends to be warmer at the C tower at the east end of the gully (blue) which is just upstream from the confluence of the gully with a major north-south gully. It is not known if the mixing of currents leads to enhanced mixing and downward heat flux. In addition, the gully becomes wider near the confluence leaving the flow more exposed to the ambient flow. The remaining stations in the gully show significant short

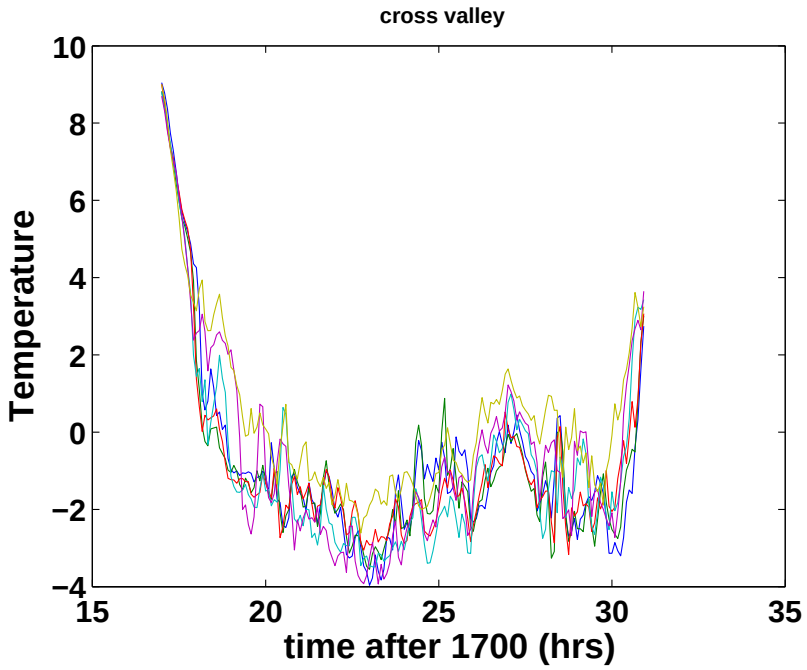

Figure 9: The along-valley variation of the 0.5 m slow-response temperature based on the C tower (blue), station 16 (green), 11 (red), 3 (cyan), 2 (violet), 1 (yellow).

term differences but no large systematic differences.

2.4 Asymmetry Indices

The wind and temperature distribution across the gully is often asymmetric. The north-facing slope may benefit from cold air descending from the southwest while the south-facing slope may receive air coming from the north that warms by mixing induced by buildings on the flat area above the slope. In addition, the cross gully ambient flow may displace the down gully flow. We will evaluate two asymmetry indices. The *thermal asymmetry* is defined simply as the average of the temperatures at stations 9 and 10 (south-facing slope) minus the average of stations 12, 13 and 14 on the north-facing slope. The thermal asymmetry (red, Figure 10) is generally positive and sometimes exceeds +2 K. The south-facing slope is warmer than the north-facing slope. It is not known if this asymmetry is influenced by greater storage of heat on

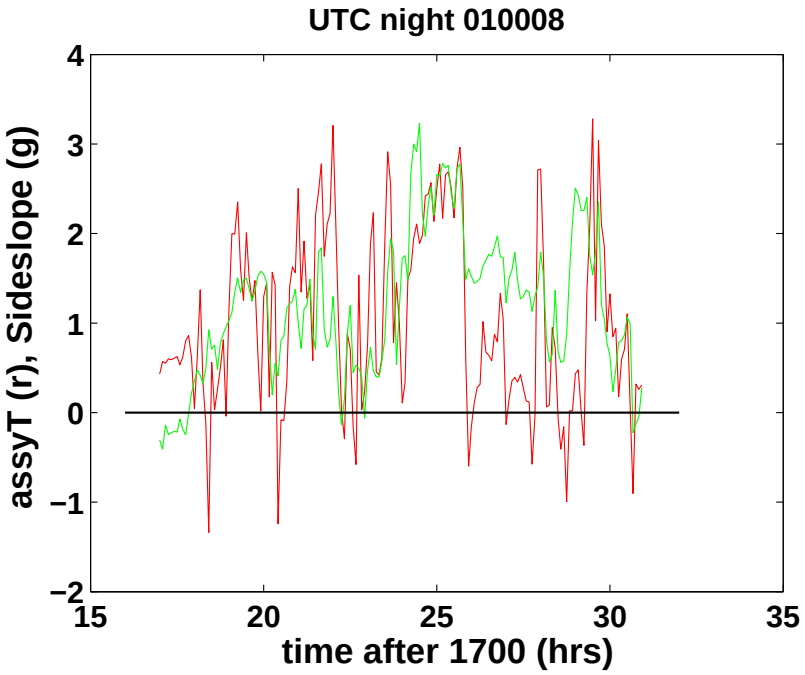

Figure 10: The cross gully thermal asymmetry (red) and wind asymmetry (green).

the south-facing slope.

The *wind asymmetry* is defined in terms of the north-south wind component using the same stations. This index (green, Figure 10) is defined such that flow down the side slopes corresponds to positive index. This index is almost always positive indicating that the side slope flow reaches the 1-m level.

An *along-valley* measure of temperature variation is defined as the temperature at the west end (station 1) minus an average of the temperature at stations 8, 11, 16 and the main tower. This index (not shown) is +3 K in the early evening and then decreases to less than unity when the wind shifts to a westerly direction and then increases again later in the evening when the westerly flow decreases again. WIth westerly flow and a larger index, the flow passing station 1 presumably flows over the colder air in the main gully, defining a cold pool. Is a cold pool in the gully more likely with north-south flow above the gully?

3 Upland gully

We now consider the behaviour of the flow at individual A stations in the early evening in the upland northern gully (stations 1, 2, 5, 6). Station A2 (Figure 11). Like the other stations, the temperature decreases rapidly in the early evening followed by a shift to westerly flow and only limited additional cooling. The vertical line identifies a cold element with a 4 C temperature drop at a little after 1900 that reaches the 1-m level but not the 2-m level and occurs with little change of speed or direction.

The upland gully stations are compared in Figure (14). The three stations in the northern gully simultaneously experience a 10-minute colder period (marked with red x's) with maximum amplitude of about a degree at A2 (green line) and weaker cooling at the upland beginning of the gully (A1, blue line) and the bottom of the gully (A5, red line). A parcel with a 1 m/s down-gully speed would require a little more than 7 minutes to travel from A1 to A5, coupled with the fact that the coldest air occurs in the longitudinal center of the gully, suggests that down-gully advection is not responsible for the temperature changes. At this time, the flow includes a southerly component so the cold element may have been advected from the southwest, as a thin layer.

The cold event does not occur at station A6 where the southern and northern gullies merge and the turbulence is stronger (not shown). The air at station 8 further down the main gully is several degrees colder, implying that the air from the northern and southern gullies overrides the air in the cold pool of the main gully. This also happens on other nights in the early evening.

At about 2 hours, the temperature drops rapidly at station 5 by almost 4 C, then at station 2 10-15 minutes later. This is the same cold element discussed in Figure 11 at Station 2. Station 1, which is more exposed to the ambient flow, also experiences substantial cooling which is more spread out in time. After this major cooling, the air temperature in the northern gully is now of comparable to the air temperature in the main gully. The air in the merging zone (station 6) is the warmest. Two related questions emerge. Why did the first cooling event occur simultaneously within the 5 min. resolution at the three stations in the northern gully? Why does the major cooling (second event) propagate to the west against the westerly wind? The two cooling events could be associated with a propagating mode that leads to deepening of the cold air through rising motion or could be associated with

the cross gully flow.

3.1 Hot spots

Transient warm air events result from bursts of turbulence and resulting downward transport of heat. Warm surface air may show preferred areas such as down wind from the buildings to the north of the domain. The confluence of the south and north gullies is intermittently warmer than surrounding stations. This needs to be explored in more detail.

4 The ambient flow

The "ambient" flow at 20 m on the tower (red +, Figure 13) is quite nonstationary and appears to significantly influence the surface flow. The 20-m flow cools only a few degrees during the night. The speed of the 20-m decreases to about 2 ms^{-1} and rotates from southerly to westerly by 2000 MST, then increases to about 6 ms^{-1} at 0300 but remains W or WNW and then again decelerates for the rest of the night. The 1-m flow at three stations outside of the gully, at roughly the same absolute height as the 20-m on the main tower, show only modest relationship to the 20-m wind flow. The flows at A1 (most western station, blue, Figure 13) and A14 (most southern station on the top of the north facing sideslope, red) are relatively well correlated. However, the flow at station 9 (green) near the top of the south-facing slope is not well correlated to the other two surface winds. The temperature at A9 is typically warmer, though not as warm as the 20-m flow. The flow at A9 is significantly more turbulent than the other two stations presumably due to the north westerly flow (after 2000) past the buildings at the top of the slope. The buildings are expected to induce mixing and downward heat flux.

The flow at the other two surface stations is more westerly or even south westerly at station 9. The latter is thought to be due to drainage of flow from the southwestern uplands just to the SW of the network.

5 Appendix

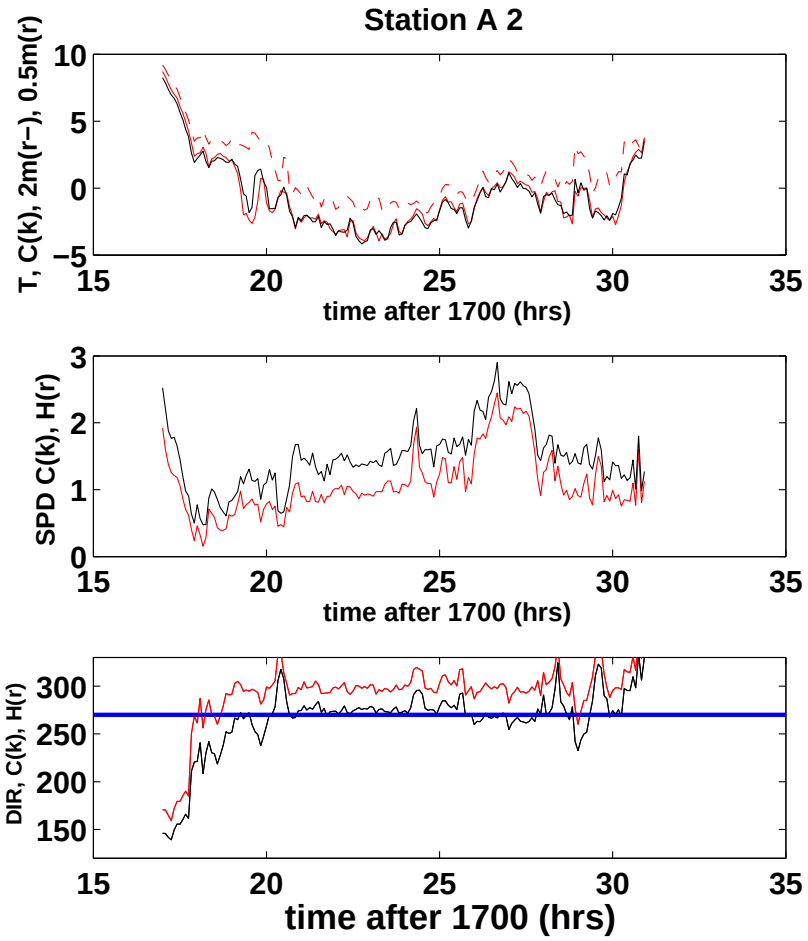

Figure 11: Time series of temperature and wind in the north gully, station A2. The upper panel records the 1-m sonic-anemometer temperature (black), the 0.5 m slow-response temperature (red) and the 2-m slow-response temperature (red dashed). The sonic-anemometer temperature may include an offset. The middle panel compares the speed of the sonic anemometer at 1 m (black) with the speed of the Handar 2-D sonic anemometer at 0.5 m (red). The bottom panel compares the wind directions of the two sonic anemometers. A final correction for wind direction has not yet been applied.

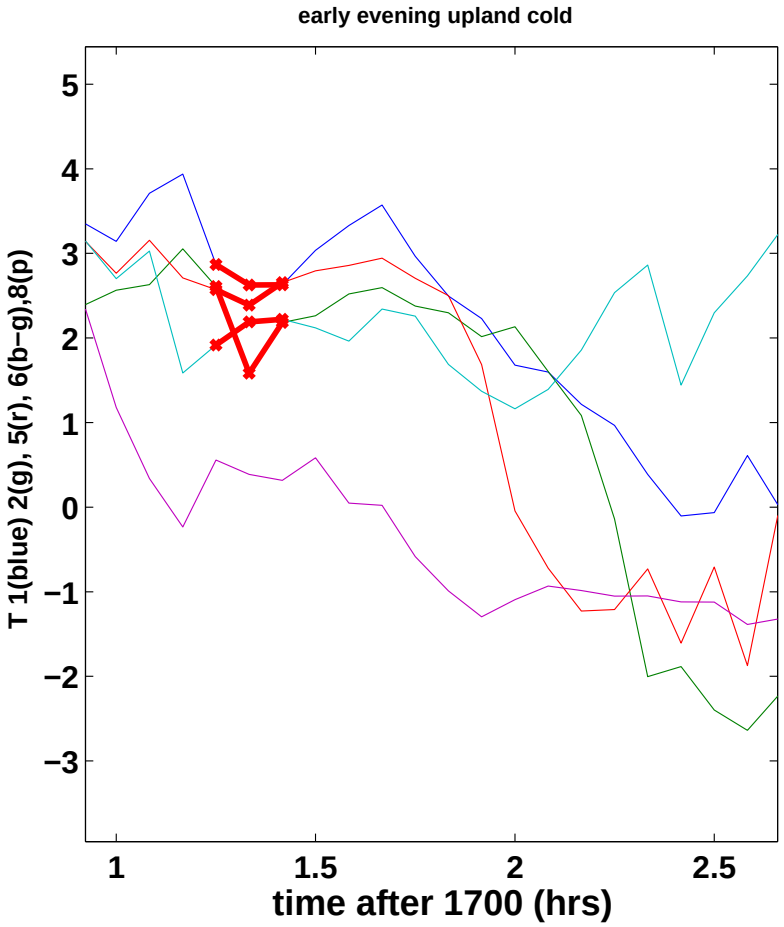

Figure 12: Temperatures at 0.5 m for A1 (blue), A2 (green), A5 (red), A6 (blue-green) and A8 (purple)

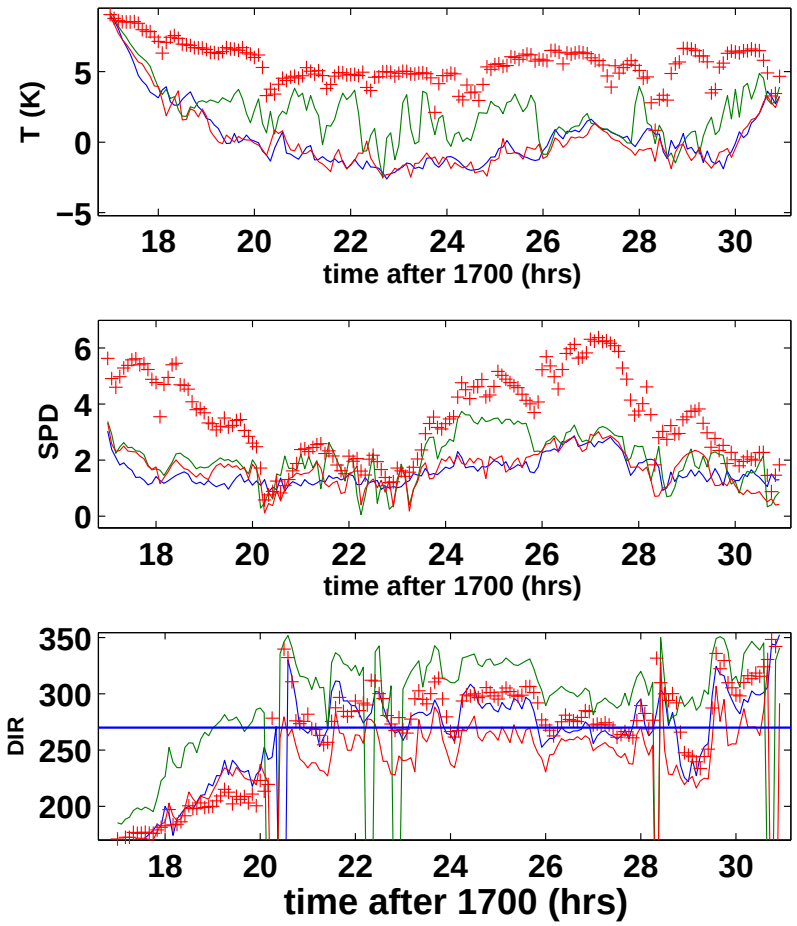

Figure 13: The temperature (upper panel), wind speed (middle panel) and wind direction (lower panel) for station A1 (blue), A9 (green), A14 (red) and the 20-m level on the main tower (red +).

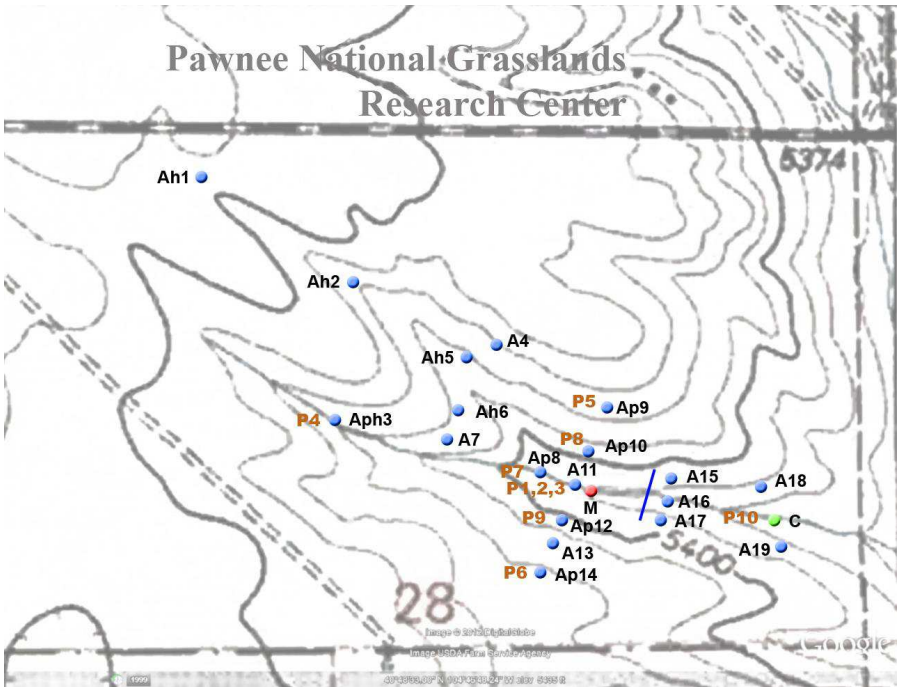

Figure 14: Map.